Numerical and Experimental Study on Topology Optimization of Fin Configuration in Latent Heat Storage

Yao Zhao[1], Hongbing Liu[1], Yin You[2] and Changying Zhao[1]

[1] Institute of Engineering Thermophysics, School of Mechanical Engineering, Shanghai Jiao Tong University, Shanghai (China)

[2] NIO Co., Ltd, Shanghai (China)

Abstract

Fin is an effective and low-cost way to enhance the heat transfer performance of latent heat storage, but its design still lacks clear theoretical guidance. In this paper, a two-dimensional model is established based on topology optimization theory in order to obtain the optimal fin configuration in the tube-and-shell latent heat storage. The effect of numerical parameters, such as mesh size, filter radius, penalty factor and objective function on the optimal fin configuration is studied. Besides, the effect of natural convection in the melting process on the optimal fin configuration is also investigated. At last, experimental validation is carried out in which the heat transfer performance of optimized fins, triangular fins and rectangular fins is compared. It is found that the optimized fins present dendritic distributions and show better heat transfer performance than other fins; numerical parameters and natural convection both have significate influence on the optimal fin configuration in latent heat storage. Topology optimization is an effective and reliable method to optimize the fin configuration in latent heat storage.

Keywords: latent heat storage, topology optimization, heat transfer, fin, experimental validation

1. Introduction

Latent heat storage is a promising way to solve the intermittence and fluctuation of renewable energy (e.g., solar energy and wind energy) and industrial waste heat, but phase change materials usually suffer from low thermal conductivity, which limits heat transfer performance of latent heat storage (Gasia et al., 2016). As a heat transfer method, fins have advantages in terms of performance stability, manufacturing feasibility, technical maturity and economy, etc. However, their structure optimization mostly relies on engineering experience and lacks clear theoretical guidance, which makes it difficult to achieve the optimal heat transfer effect.

Topology optimization can realize the high degree of freedom structure optimization under specific objectives. So far, it has been widely applied in the field of mechanics (Eschenauer and Olhoff, 2001) and began to extend to the field of flow and heat transfer, e.g., fin structure optimization (Alexandersen et al., 2016; Joo et al., 2017) and flow channel design (Dilgen et al., 2018; Gersborg-Hansen et al., 2005) in the heat sink. As for latent heat storage, Pizzolato et al. (2017a, b; 2019) first introduced topology optimization theory into the design of fin configuration in the tube-and-shell latent heat storage and investigated the effect of natural convection, material selection, flow arrangements and design constraints on the optimal fin configurations. You et al.(2019) obtained and reconstructed the optimized fins by topology optimization and then compared the optimized fins and other typical types of fins through CFD simulation. However, the effect of numerical parameters on the optimal fin configuration in latent heat storage is not fully discussed. In addition, the experimental study and validation still have not been carried out for the topology optimization of fin configurations in latent heat storage.

In this study, a two-dimensional model is established based on topology optimization theory in order to optimize the fin configuration in the tube-and-shell latent heat storage. The effect of numerical parameters, such as mesh size, filter radius, penalty factor and objective function on the optimal fin configuration is studied.

doi:10.18086/swc.2019.22.09 Available at http://proceedings.ises.org

Besides, the effect of natural convection in the melting process on the optimal fin configuration is also investigated. Experimental study is carried out in which heat transfer performance and phase change process with optimized fins, triangular fins and rectangular fins are compared.

2. Model description

2.1 Physical model

Fig.1 shows the simplified two-dimensional model of tube-and-shell latent heat storage where the right half of the cross section is taken as the design domain due to the symmetry. The design domain consists two parts: phase change materials, Ω_{PCM} and heat conduction materials, Ω_{HCM}. r_1 and r_2 are the radii of heat transfer tube and storage tank, respectively. The inner and outer walls are regarded as constant temperature boundary and adiabatic boundary, respectively. In this study, r_1 and r_2 equal to 0.02m and 0.05m, respectively. The temperature at inner wall, T_b, is 373K. Paraffin RT60 and aluminum are used as PCMs and HCMs, respectively, with a volume ratio of PCMs being 15%. The thermophysical parameters of PCMs and HCMs are listed in Tab.1. The initial temperature of the whole domain is 298.15K.

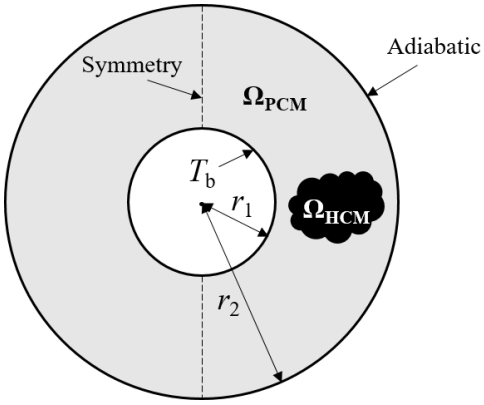

Fig. 1: Physical model of latent heat storage

Tab. 1: Thermophysical parameters of PCMs and HCMs

Parameter	Value
Density of PCMs, ρ_{PCM}	780 kg/m^3
Density of HCMs, ρ_{HCM}	2700 kg/m^3
Thermal conductivity of PCMs, k_{PCM}	0.15 W/(m·K)
Thermal conductivity of HCMs, k_{HCM}	214 W/(m·K)
Specific heat capacity of PCMs, $c_{p,PCM}$	2120 J/(kg·K)
Specific heat capacity of HCMs, $c_{p,HCM}$	891 J/(kg·K)
Viscosity of PCMs, μ	0.0039 Pa·s
Coefficient of thermal expansion, β	0.002 K^{-1}
Melting temperature, T_m	333.15 K
Melting temperature range, T_1/T_2	323.15 K/343.15 K
Latent heat of PCMs, L	200 kJ/kg

2.2 Mathematical model

2.2.1 Governing equation

Continuity equation

$$\frac{\partial u}{\partial x}+\frac{\partial v}{\partial y}=0 \qquad \text{(eq. 1)}$$

Momentum equation

$$\frac{\partial u}{\partial t}+u\frac{\partial u}{\partial x}+v\frac{\partial u}{\partial y}=-\frac{1}{p}\frac{\partial p}{\partial x}+\mu\left(\frac{\partial^2 u}{\partial x^2}+\frac{\partial^2 u}{\partial y^2}\right)-\alpha(x)u \qquad \text{(eq. 2)}$$

$$\frac{\partial v}{\partial t}+u\frac{\partial v}{\partial x}+v\frac{\partial v}{\partial y}=-\frac{1}{p}\frac{\partial p}{\partial y}+\mu\left(\frac{\partial^2 v}{\partial x^2}+\frac{\partial^2 v}{\partial y^2}\right)-\alpha(x)v-g\beta(T-T_0) \qquad \text{(eq. 3)}$$

The terms $\alpha(x)u$ and $\alpha(x)v$ are brinkman terms to distinguish PCMs and HCMs as well as solid phase and liquid phase of PCMs. Term $g\beta(T\text{-}T_0)$ is the Boussinesq approximation to describe the natural convection in liquid PCMs. $\alpha(x)$ is defined as following:

$$\alpha(x)=\begin{cases}\alpha_{\mathrm{HCM}}\gg 1, & \rho_{\mathrm{s}}(x)=1\\ \alpha_{\mathrm{PCM}}(T), & \rho_{\mathrm{s}}(x)=0\end{cases} \qquad \text{(eq. 4)}$$

$$\alpha_{\mathrm{PCM}}(T)=\begin{cases}\alpha_{\mathrm{PCM,liquid}}, & T>T_{\mathrm{m}}\\ \alpha_{\mathrm{PCM,solid}}, & T\le T_{\mathrm{m}}\end{cases} \qquad \text{(eq. 5)}$$

Energy equation

$$\left(\rho c_{\mathrm{p}}+\rho L(T)\right)\frac{\partial T}{\partial t}+\left(\rho c_{\mathrm{p}}+\rho L(T)\right)\left(\frac{\partial(uT)}{\partial x}+\frac{\partial(vT)}{\partial y}\right)=\frac{\partial}{\partial x}\left(k(x)\frac{\partial T}{\partial x}\right)+\frac{\partial}{\partial y}\left(k(x)\frac{\partial T}{\partial y}\right) \qquad \text{(eq. 6)}$$

Here, $L(T)$ is defined as the function of temperature T and satisfies the following equations:

$$\int_{T_1}^{T_2}L(T)dT=L \qquad \text{(eq. 7)}$$

$$L(T)=\begin{cases}0, T\in(0,T_1]\cup[T_2,+\infty)\\ A_1(T-T_1), T\in(T_1,T_{\mathrm{m}})\\ A_2(T-T_2), T\in(T_{\mathrm{m}},T_2)\end{cases} \qquad \text{(eq. 8)}$$

where $T\in(T_1, T_2)$ is the range for phase change, A_1 and A_2 are constants for the latent heat curve.

2.2.2 Boundary and initial condition

The inner and outer walls are both impermeable and no-slip.

$$u=v=0 \qquad \text{(eq. 9)}$$

The inner wall is set to a specific temperature T_{b} higher than melting temperature T_{m}.

$$T=T_{\mathrm{b}}=373\mathrm{K} \qquad \text{(eq. 10)}$$

The outer wall is adiabatic.

$$q=0 \qquad \text{(eq. 11)}$$

The initial temperature of the whole design domain is 298.15K.

$$T=298.15\mathrm{K} \qquad \text{(eq. 12)}$$

2.2.3 Topology optimization:

The mathematical model of topology optimization can be expressed as follows:

Objective $\quad$ Maximum $z_1(T(x),x)=\frac{\int_\Omega T(x)dx}{V}$ or $z_2(h(x),x)=\int_\Omega h(x)dx \qquad \text{(eq. 13)}$

Constraints $\quad F(u(x),v(x),T(x),x)=0 \qquad \text{(eq. 14)}$

$$\int_\Omega \rho dV\le\Phi\int_\Omega dV \qquad \text{(eq. 15)}$$

$$x \in X = \{x_1, x_2, x_3 \ldots x_N\} \qquad \text{(eq. 16)}$$

The optimization objective in this paper is to maximum the average temperature or the total enthalpy of the whole domain within a fixed time *t*. The constraint (eq. 14) is the governing equation and the constraint (eq. 15) is used to limit the volume ratio of HCMs. SIMP method is used to define the design variables, which distinguish PCMs and HCMs. In the SIMP method, penalty factor *p* is defined to realize the 0-1 distribution of design variables. The thermophysical parameters are redefined as follows:

$$k(x) = k_{\mathrm{PCM}} + \rho_{\mathrm{s}}^{p}(k_{\mathrm{HCM}} - k_{\mathrm{PCM}}) \qquad \text{(eq. 17)}$$

$$\rho(x) = \rho_{\mathrm{PCM}} + \rho_{\mathrm{s}}(\rho_{\mathrm{HCM}} - \rho_{\mathrm{PCM}}) \qquad \text{(eq. 18)}$$

$$c_{\mathrm{p}}(x) = c_{\mathrm{p,PCM}} + \rho_{\mathrm{s}}(c_{\mathrm{p,HCM}} - c_{\mathrm{p,PCM}}) \qquad \text{(eq. 19)}$$

$$L(x) = (1 - \rho_{\mathrm{s}})L \qquad \text{(eq. 20)}$$

$$\alpha(x) = \alpha_{\mathrm{PCM}}(T) + \rho_{\mathrm{s}}(\alpha_{\mathrm{HCM}} - \alpha_{\mathrm{PCM}}(T)) \qquad \text{(eq. 21)}$$

2.2.4 Numerical methodology

Finite element method is used to discrete the governing equations and MMA is used as the optimization method in each iteration. Whether the momentum equations are solved depends on whether the flow in liquid PCMs is considered. Besides, Helmholtz-type differential equation is solved as a filter method in order to ensure the convergence:

$$\nabla \cdot (-r_{\mathrm{f}}\nabla\rho_{\mathrm{f}}) + \nabla\rho_{\mathrm{f}} = \rho_{\mathrm{s}} \qquad \text{(eq. 22)}$$

where r_{f} and ρ_{f} are filter radius and design parameter after filter, respectively. The convergence criteria are all 1×10^{-6}.

3. Experimental system

Fig.2 shows the experimental systems. In Fig.2(a), the oil bath supplies constant-temperature oil to the test module as a constant-temperature heat source. The temperature of the oil supplied by the oil bath is fixed at 90℃. The oil temperatures at the inlet and outlet of the test module, the PCM temperature inside the test module, and the flow rate of the oil are measured and recorded. In Fig.2(b), the tube and fins are sealed in a quartz glass container. During the experiment, the heat oil is stored in the tube and the space between fins and quartz glass is filled with Paraffin RT60. Six K-type thermocouples are inserted into the quartz glass container to measure the temperature of PCMs as shown in Fig.2(b). Three kinds of aluminum fins (the optimized fins, the triangular fins and the rectangular fins) are manufactured by wire-electrode cutting and then are sealed in test modules, respectively. The three kinds of fins have the same volume. The optimized fins, the triangular fins and the rectangular fins are shown in Fig.3, respectively.

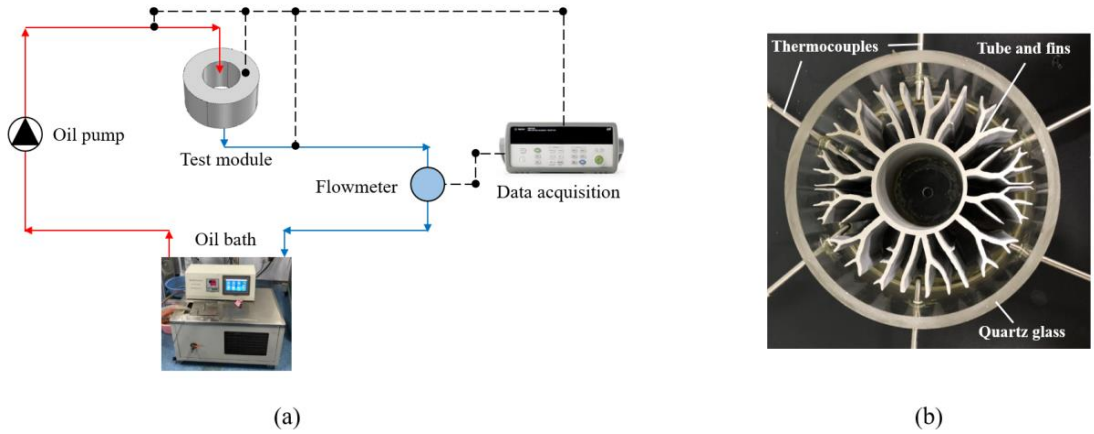

Fig. 2: Experimental system

Fig. 3: Three kinds of fin configurations adopted in the experiment

4. Results and discussion

4.1 Effect of numerical parameters

4.1.1 Mesh size

Three different mesh sizes (0.0015mm, 0.001mm and 0.0008mm) are compared in which the flow in liquid PCMs is neglected and the optimization objective is to maximum the average temperature of the whole domain within t=300s. Fig.4 shows the effect of mesh size on the fin configuration in which the left half is the mesh and the right half is the fin configuration. It is found that the fins show similar dendritic distributions under different mesh sizes. When mesh size is 0.0015mm, it is obvious that there exists discontinuity in the fin structure. As the mesh size decreases, the fin structure becomes more sophisticated with sharper boundaries. When mesh size decreases to 0.001mm, no obvious difference exists in fin configurations compared with smaller mesh sizes, thus the mesh size of 0.001mm is adopted in the following study.

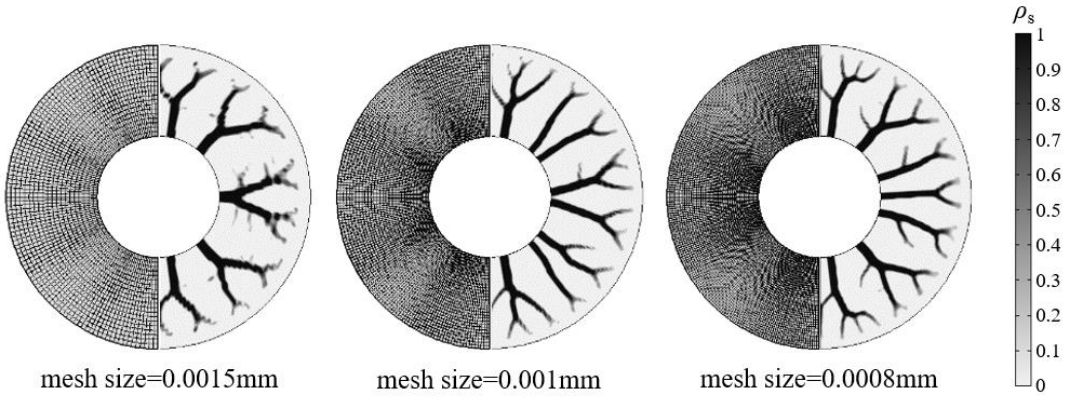

Fig. 4: Effect of mesh size on the fin configuration

4.1.2 Filter radius

Three different filter radii (0.0003mm, 0.0005mm and 0.0008mm) are compared in which the flow in liquid PCMs is neglected and the optimization objective is to maximum the average temperature of the whole domain within t=300s. Fig.5 shows the effect of filter radius on the optimal fin configuration. It is found that though larger filter radius r_f can effectively alleviate the discontinuity and checkerboard of fin configuration, the fuzzy area of fin structures is larger and more details of the fin structures are lost with filter radius r_f increasing.

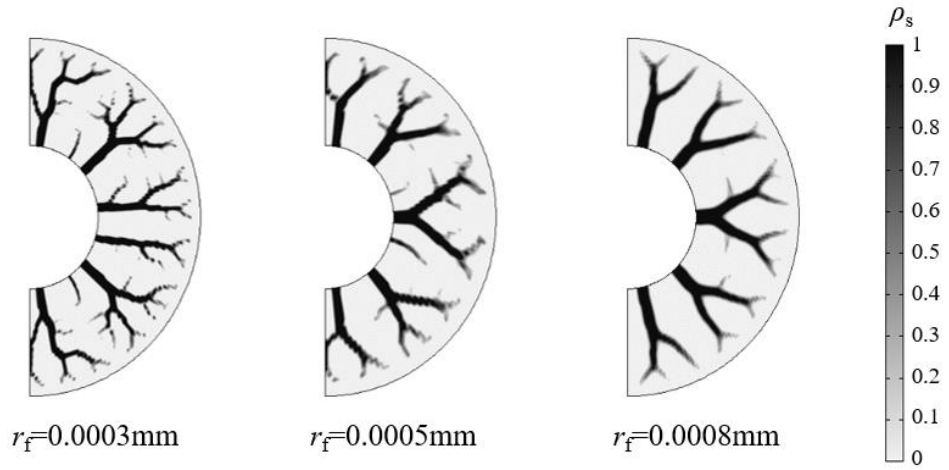

Fig. 5: Effect of filter radius on the fin configuration

4.1.3 Penalty factor

Three different penalty factors (3, 4 and 5) are compared in which the flow in liquid PCMs is neglected and the optimization objective is to maximum the average temperature of the whole domain within *t*=300s. Fig.6 shows the effect of penalty factor on the optimal fin configuration. It is shown that smaller penalty factor reduces the penalty effect on the intermediate value of the design variable Φ, thus leading to more dispersed structures and fuzzy areas.

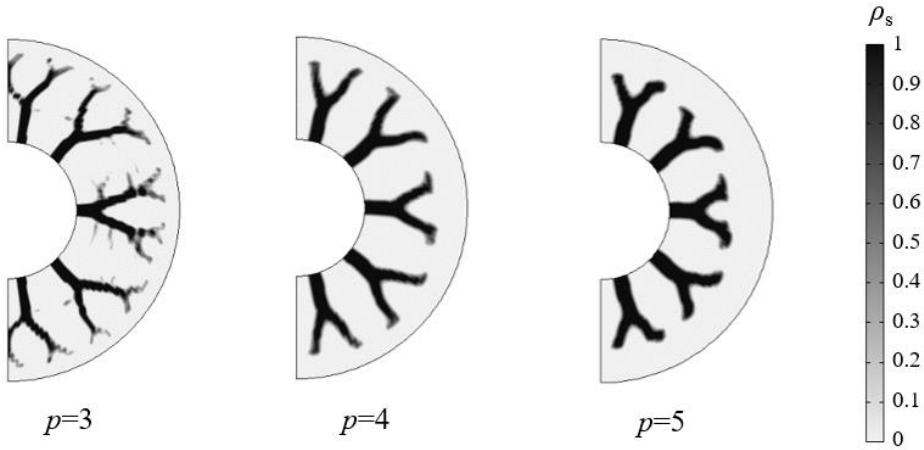

Fig. 6: Effect of penalty factor on the fin configuration

4.1.4 Objective function

Two different objective functions (maximizing the average temperature and the total enthalpy in 300s) are compared in which the flow in liquid PCMs. Fig.7 shows the effect of objective functions on the fin configuration in which the left half is the fin configuration and the right half is the temperature distribution at *t*=300s. It is found that the fin configuration both show similar dendritic distributions under different objective function. When the objective is to maximize the average temperature, the fins are distributed uniformly in shape and size, thus leading to a uniform temperature field. But when the objective changes to maximize the total enthalpy, the fins in the upper and lower parts are large than those in the middle part, which leads to a non-uniform temperature field.

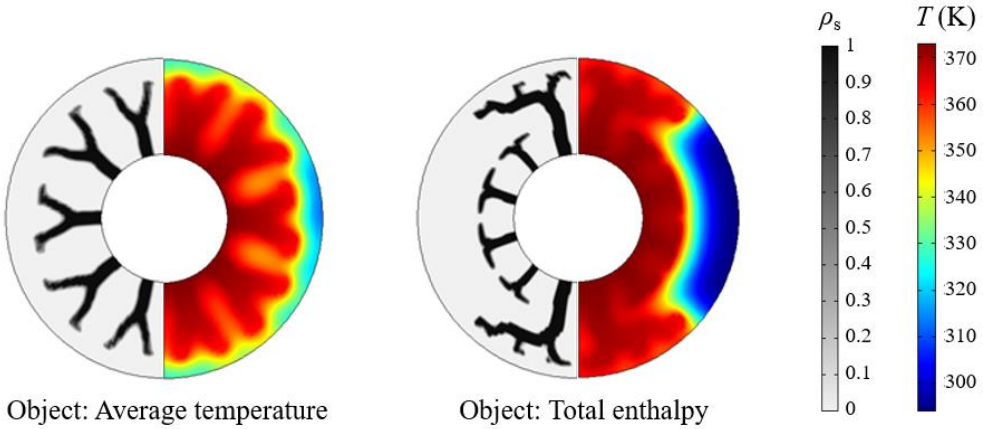

Fig. 7: Effect of objective function on the fin configuration

4.2. Effect of natural convection

Fig.8 shows the effect of natural convection in melting process on the optimal fin configuration and the corresponding temperature/ flow field distributions. Due to natural convection, liquid PCMs heated by the hot tube usually flow upward continuously and forms a closed flow loop in the cavity, which will promote the heat charging process. Uniform-distributed fin configuration tends to suppress the flow in the cavity. In Fig.8, when natural convection in liquid PCMs is taken into consideration, the fins in the middle part are much shorter than those in the upper and lower parts, which forms an internal circulation flow and promotes heat transfer in melting process. From the beginning to t=100s, PCMs absorb heat from the fins and natural convection tends to be strong. After t=100s, natural convection begins to weaken.

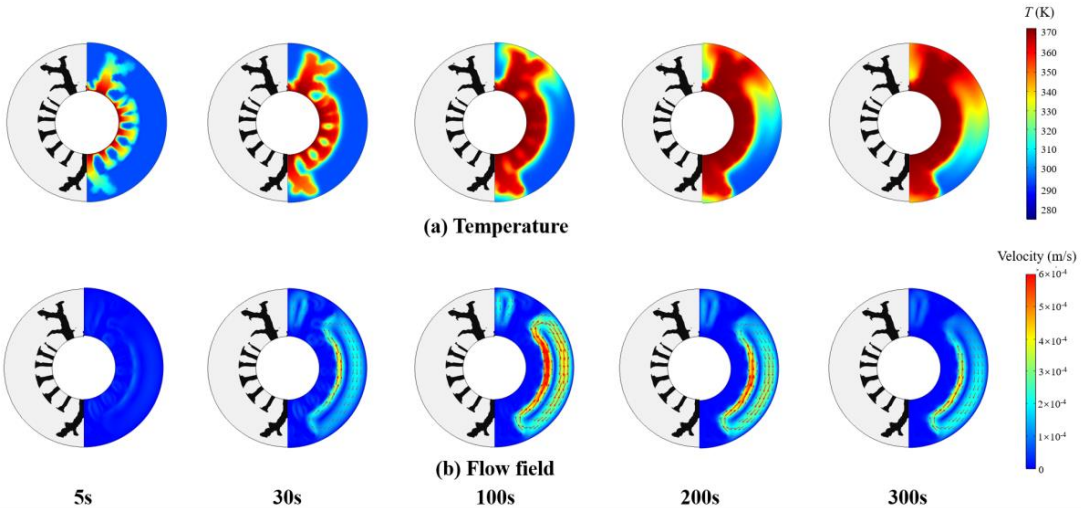

Fig. 8: Effect of natural convection on the fin configuration

4.3 Experimental validation

In the previous studies, the optimized fins, the triangular fins and the rectangular fins are reconstructed through CAD methods and their performance has been compared by CFD simulation (You et al., 2019). In this paper, the experiment is carried out to validate the excellent heat transfer performance of the fins obtained by topology optimization. Fig.9 shows the average temperatures of PCMs with different fin configurations. The PCM temperature increases fastest and melting finishes at about t=17min with optimized fins. As for triangular and rectangular fins, the average temperatures reach melting temperature at t=20.5min and t=23min, respectively. At t=17min, the average temperature of PCMs with optimized fins is 20K higher than those of PCMs with triangular and rectangular fins. Besides, compared with the simulation results, the temperature evolution

obtained by experiment lags behind, because no insulation measures are taken for the test module.

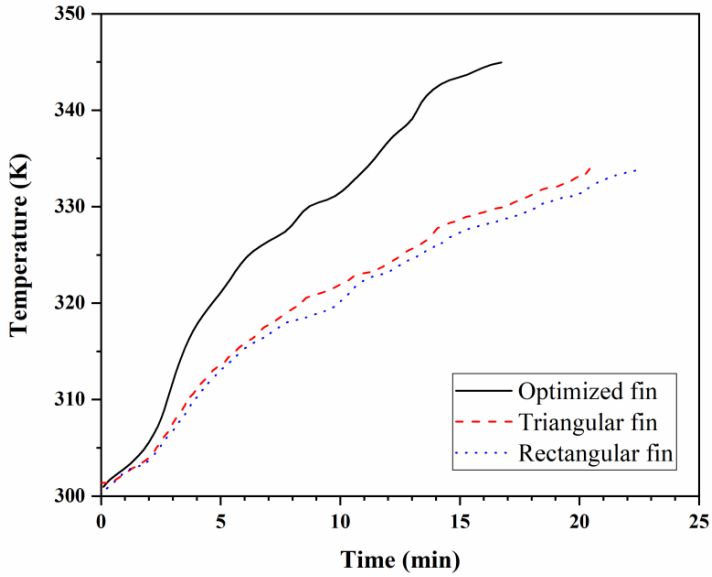

Fig. 9: Comparison of average temperatures of PCMs with different fin configurations

In Fig.10, it is obviously shown that there is still a large amount of PCMs remaining solid state with triangular and rectangular fins when PCMs completely melt with optimized fins.

Fig. 10: Comparison of liquid fraction of PCMs with different fin configurations

5. Conclusions

In this paper, the topology optimization of fin configuration in latent heat storage is carried out. The effect of numerical parameters, such as mesh size, filter radius, penalty factor and objective function on the optimal fin configuration is studied. Besides, the effect of natural convection in the melting process on the optimal fin configuration is also investigated. At last, experimental validation is performed. The main conclusions are drawn as follows:

- Optimized fins show dendritic distributions and numerical parameters have significate influence on the optimal fin configuration in latent heat storage. Mesh size and filter radius are related to the discontinuity of the fin configuration. Filter radius and penalty factor affect the distribution of the design variable at the interfaces.
- Natural convection leads the fins in the middle part to be shorter than those in the upper and lower part, thus forming a closed flow loop and promoting the heat transfer.
- The better heat transfer performance of the optimized fins obtained by topology optimization is validated by experiment. Topology optimization is an effective and reliable method to optimize the fin configuration in latent heat storage.

6. Acknowledgments

This work is supported by the National Key Basic Research Program of China (973 Project: 2013CB228303) and the National Natural Science Foundation of China (Grant No.51906150).

7. References

Alexandersen, J., Sigmund, O., Aage, N., 2016. Large scale three-dimensional topology optimisation of heat sinks cooled by natural convection. International Journal of Heat and Mass Transfer 100, 876-891.

Dilgen, S.B., Dilgen, C.B., Fuhrman, D.R., Sigmund, O., Lazarov, B.S., 2018. Density based topology optimization of turbulent flow heat transfer systems. Struct Multidiscip O 57(5), 1905-1918.

Eschenauer, H.A., Olhoff, N., 2001. Topology optimization of continuum structures: A review. Applied Mechanics Reviews 54(4), 331-390.

Gasia, J., Miró, L., Cabeza, L.F., 2016. Materials and system requirements of high temperature thermal energy storage systems: A review. Part 2: Thermal conductivity enhancement techniques. Renewable and Sustainable Energy Reviews 60, 1584-1601.

Gersborg-Hansen, A., Sigmund, O., Haber, R.B., 2005. Topology optimization of channel flow problems. Struct Multidiscip O 30(3), 181-192.

Joo, Y., Lee, I., Kim, S.J., 2017. Topology optimization of heat sinks in natural convection considering the effect of shape-dependent heat transfer coefficient. International Journal of Heat and Mass Transfer 109, 123-133.

Pizzolato, A., Sharma, A., Ge, R., Maute, K., Verda, V., Sciacovelli, A., 2019. Maximization of performance in multi-tube latent heat storage-Optimization of fins topology, effect of materials selection and flow arrangements. Energy.

Pizzolato, A., Sharma, A., Maute, K., Sciacovelli, A., Verda, V., 2017a. Design of effective fins for fast PCM melting and solidification in shell-and-tube latent heat thermal energy storage through topology optimization. Applied Energy 208, 210-227.

Pizzolato, A., Sharma, A., Maute, K., Sciacovelli, A., Verda, V., 2017b. Topology optimization for heat transfer enhancement in Latent Heat Thermal Energy Storage. International Journal of Heat and Mass Transfer 113, 875-888.

You, Y., Zhao, Y., Zhao, C., Liu, H., 2019. The topology optimization of the fin structure in latent heat storage. Chinese Science Bulletin 64, 1191-1199.